Instabilities of Sheared Flow in an Idealized Arctic-Ocean Gyre Model

Rosalie Cormier, Francis Poulin, Andrea Scott

Department of Applied Mathematics, University of Waterloo

Acknowledgements

This research is supported by funding from the Province of Ontario (via Ontario Graduate Scholarships), the Natural Sciences and Engineering Research Council of Canada (via the CREATE program), and the University of Waterloo.

Motivation: Beaufort Gyre energetics

Beaufort Gyre: A region of wind-driven circulation in the Arctic Ocean.

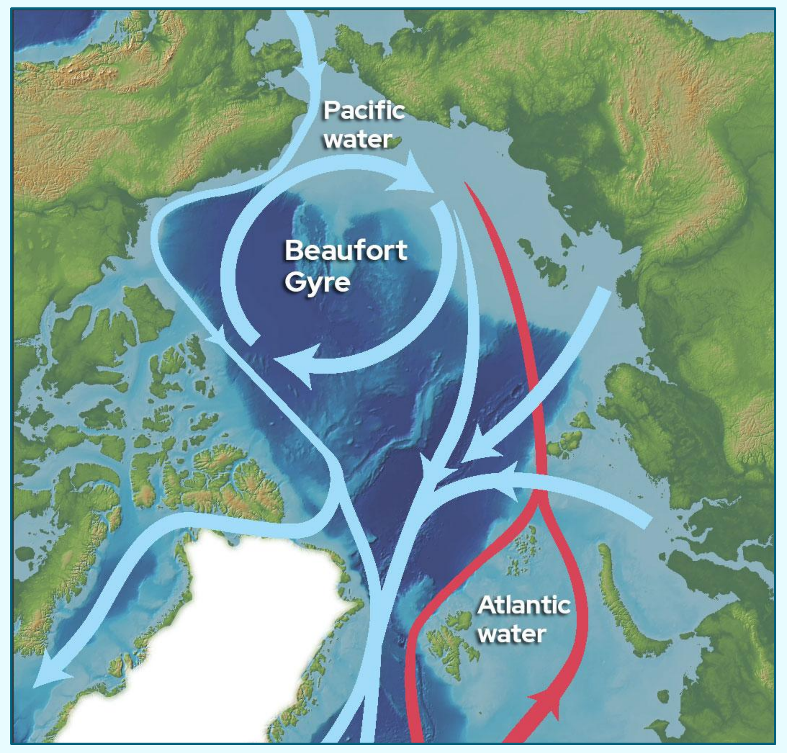

Fig. 1: Schematic of Arctic Ocean circulation. From [1].

Wind-to-water momentum transfer maintains **sheared flow** in the gyre, balanced by bowl-shaped isopycnal surfaces.

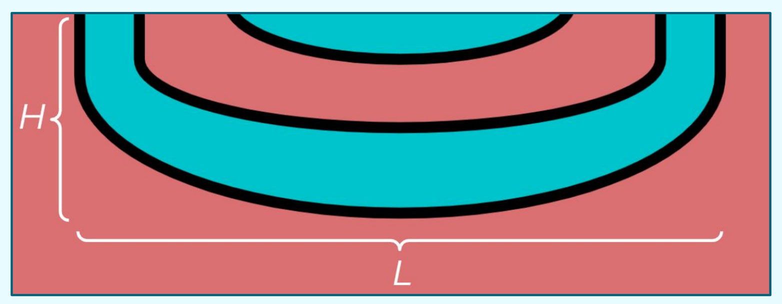

Fig. 2: Schematic of Beaufort Gyre's radial and vertical structure. Colours represent alternating temperatures of water masses (blue – cold; red – warm). Black lines represent isopycnals (buoyancy contours). Length scales L ~ 500 km and H ~ 500 m are labelled. Flow velocity is perpendicular to the page and clockwise as viewed from above the gyre.

Salinity sets Arctic water density, allowing warm water to remain at depth.

- Concave isopycnals signify **available potential energy (APE)**: potential energy that is available for conversion into other forms of energy

Strong, stable background stratification inhibits vertical motion.

- If the gyre's velocity profile is dynamically **unstable**, small perturbations may amplify until nonlinear saturation occurs
  - Nonlinear interactions produce turbulent **eddies** that weaken the gyre's stratification; vertical transports (*e.g.*, of warm water) become more energetically accessible

Primitive equations and linearization

I. Assumptions:

- *L*, *H* are much smaller than planetary radius [2]
- Boussinesq approximation (density fluctuations are small)
- No thermodynamic buoyancy sources
- Inviscid limit

$$\frac{D\vec{u}}{Dt} = -f\hat{z}\times\vec{u} - \frac{1}{\rho_0}\nabla p + b\hat{z} \quad \text{(1a)}$$
$$\nabla\cdot\vec{u} = 0 \quad \text{(1b)}$$
$$\frac{Db}{Dt} = 0. \quad \text{(1c)}$$

II. Decompose primitive fields into steady background fields and evolving perturbation fields:

$$\vec{u}(\vec{x},t) = \vec{U}(\vec{x}) + \vec{u}'(\vec{x},t) \quad \text{(2a)}$$
$$p(\vec{x},t) = P(\vec{x}) + p'(\vec{x},t) \quad \text{(2b)}$$
$$b(\vec{x},t) = B(\vec{x}) + b'(\vec{x},t) \quad \text{(2c)}$$

III. Motivated by the Beaufort Gyre, assume an azimuthal background flow in geostrophic and hydrostatic balance. In cylindrical coordinates,

$$\vec{U} = U(r,z)\hat{\phi} \quad \text{(3a)}$$
$$\frac{1}{\rho_0}\nabla P = -f\hat{z}\times\vec{U} + B\hat{z} \quad \text{(3b)}$$

IV. Linearize (1) around background state (3) and assume a normal-mode solution:

$$[\vec{u}', p', b'](r,\phi,z,t) = \mathrm{Re}\{[\hat{\vec{u}},\hat{p},\hat{b}](r,z)\exp(ik(\phi - c_k t))\} \quad \text{(4)}$$

This yields a **generalized eigenvalue problem** with generalized eigenvalue c_k.

- Generalized eigenvectors are **spatial structures** of perturbation modes
- The product $c_k k = \omega$ determines:
  - Phase speed (Re{ω}) of the k^{th} mode
  - Temporal **growth rate** (Im{ω}) of the k^{th} mode

Sources of perturbation kinetic energy (pKE)

Time-evolution of total pKE (fixed domain with no energy transfer through boundaries, by analogy with Pedlosky [3]):

$$\frac{d}{dt}\iiint_{\mathcal{V}}\left(\frac{\vec{u}'\cdot\vec{u}'}{2}\right)dV = \underbrace{\iiint_{\mathcal{V}} b'u_z'\,dV}_{(i)} - \underbrace{\iiint_{\mathcal{V}}\frac{\partial U_\phi}{\partial r}u_r'u_\phi'\,dV}_{(ii)} - \underbrace{\iiint_{\mathcal{V}}\frac{\partial U_\phi}{\partial z}u_\phi'u_z'\,dV}_{(iii)} \quad (5)$$

(i) APE *of the perturbation* is converted to pKE

(ii) **Barotropic-instability** term: KE associated with **horizontal shear** of background flow is transferred to the perturbation

(iii) **Baroclinic-instability** term: APE associated with **vertical shear** of background flow is converted to pKE

Per Rayleigh's theorems, our idealization of the Beaufort Gyre's background flow is susceptible to development of both barotropic and baroclinic instabilities [4].

A relevant dimensionless parameter is the **Burger number**:

$$\mathrm{Bu} \equiv \frac{N^2H^2}{f^2L^2} \quad (6)$$

- Bu >> 1: expect pKE to grow mainly by barotropic instability [5]
- Bu << 1: expect pKE to grow mainly by baroclinic instability [5]

Linear stability computations

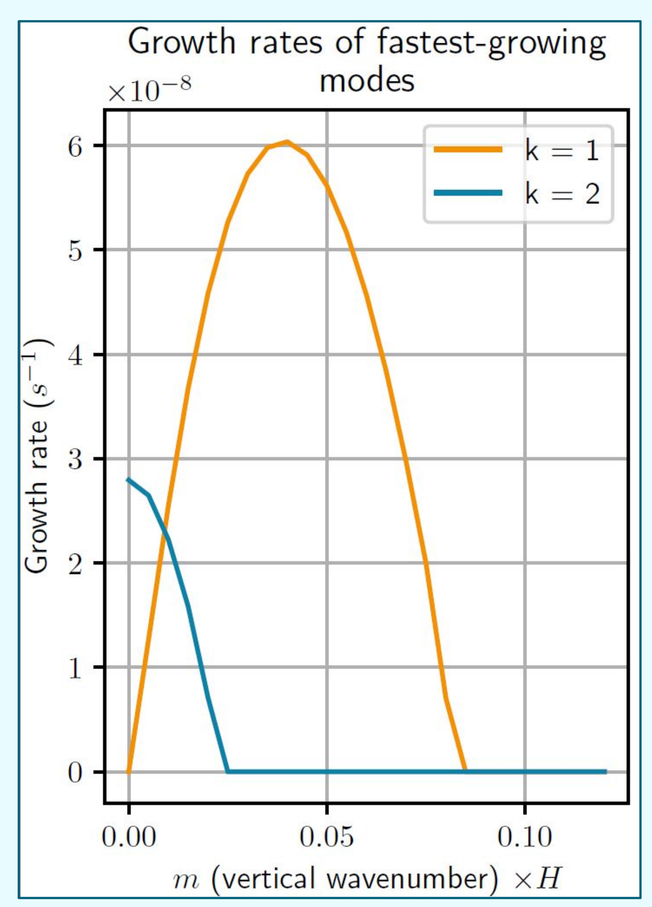

Fig. 3 (above): Computed growth rates for k = 1, 2, plotted against vertical wavenumber.

We use numerical methods for eigenvalue computation (following Storer *et al.* [5]) to obtain the spectrum of the generalized eigenvalue problem (4) for an idealized gyre-like background state.

Our preliminary computations:

- Solve the linearized **quasi-geostrophic (QG)** equations
  - Computationally lighter: solve only for streamfunction ψ, instead of 5 primitive variables
- Use constant background N^2 and $U(r, z) = U(r)$
  - Reduces dimensionality: assumes modal structure in *z* as well, so eigenvectors depend on *r* only
- Have Bu = 2.5×10^{-3}

Fig. 4 (below): Cross-section of real part of fastest-growing computed streamfunction for each of k = 1, 2.

Consistent with published linear stability analyses (*e.g.*, [4, 5]), *k* = 1, 2 have unstable modes.

- Fastest growth with *k* = 1 is for a **baroclinic mode**: periodic with depth
- Fastest growth with *k* = 2 is for **barotropic mode**: constant with depth
  - This mode is less radially confined than the former

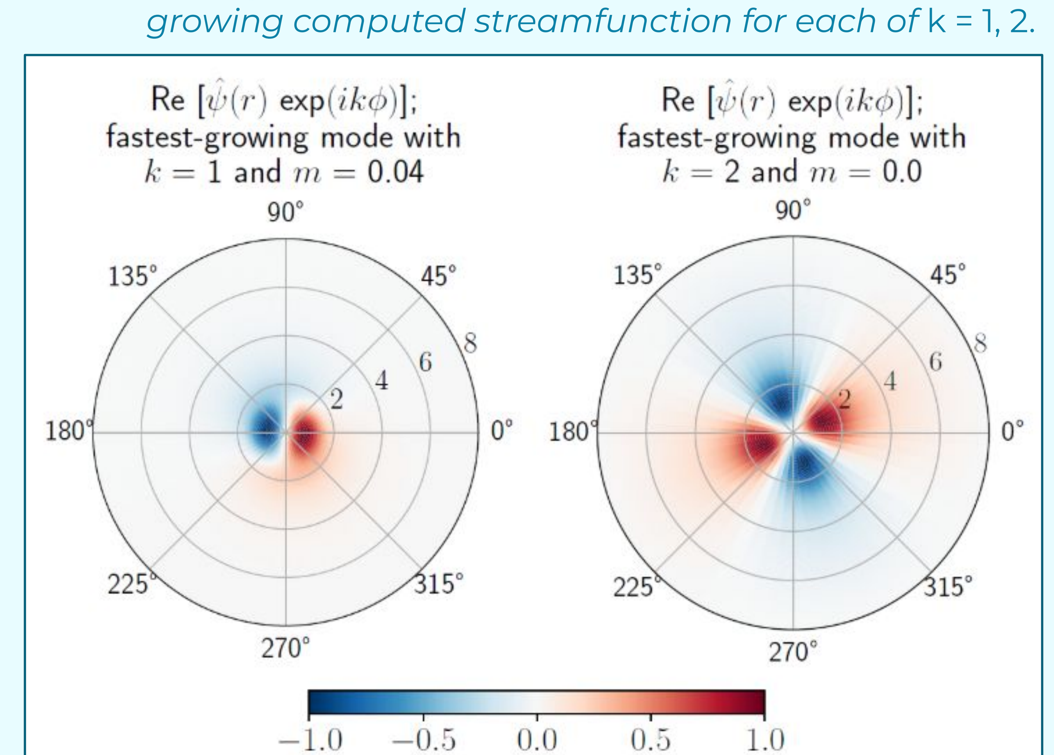

Comparison with nonlinear simulations

We evolve the nonlinear primitive equations (1) using the Oceananigans.jl library for **finite-volume** ocean simulations [6].

- Numerically diffusive, 5th-order upwinding advection scheme
- Random initial perturbation is added to balanced background flow

Simulation output shows pronounced **exponential growth** in primitive fields and evidence of subsequent **nonlinear saturation**.

- Simulation requires an unrealistically large domain (1000 km x 1000 km in the horizontal) to accommodate fastest-growing mode (see Fig. 4)

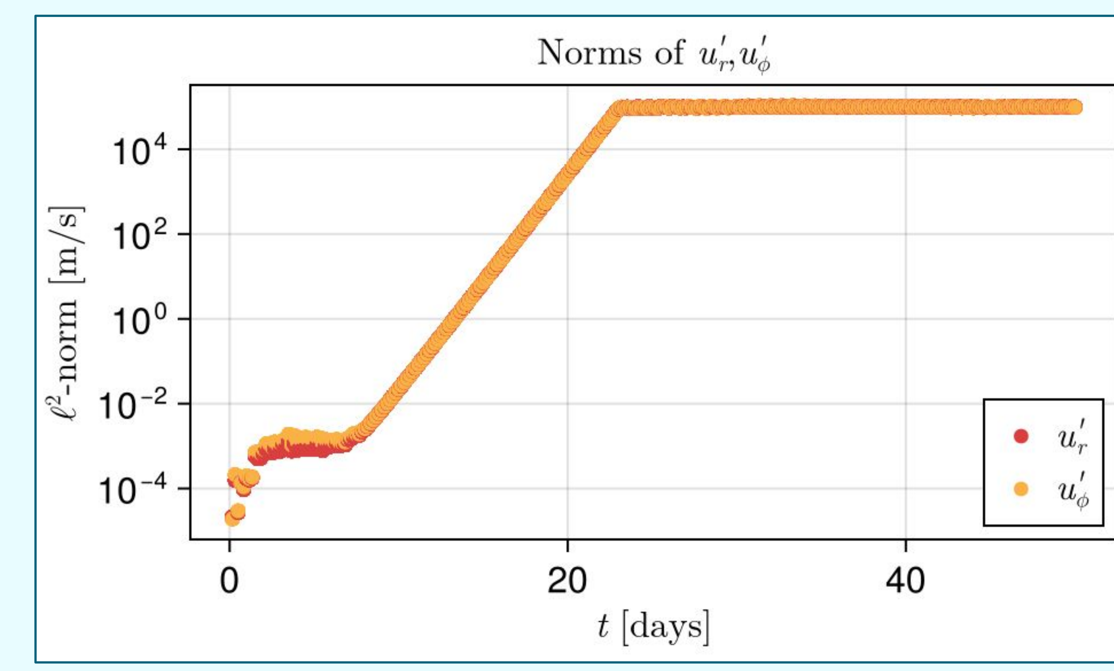

Fig. 5: ℓ^2-norms of horizontal-velocity components during initial 50 days of simulation time.

Least-squares fits of the (logarithm of) the above norms, during the regime of exponential growth, to linear functions, reveal **empirical growth rates** on the order of 10^{-6} s^{-1} for both u_r' and u_ϕ'.

- Our linear stability computations **underestimate** the maximum growth rate of the perturbation in our nonlinear simulation

Future work

- Further investigate discrepancies between empirical growth rates and growth rates obtained from linear stability computations
- Compute contributions to pKE budget, equation (5)
- Account for realistic stratification in linear stability computations and nonlinear simulations; solve both for a baroclinic background state
- Complete linear stability computations for full primitive equations
  - Relaxing the QG assumptions will allow us to study instabilities on a wider range of spatial scales
- Incorporate effects of dynamical surface forcing by winds and sea ice into nonlinear simulation

References

[1] Woods Hole Oceanographic Institution (accessed 2025). *Beaufort Gyre Exploration Project*.
[2] Vallis, G.K. (2017). *Atmospheric and Oceanic Fluid Dynamics*. Cambridge University Press.
[3] Pedlosky, J. (1987). *Geophysical Fluid Dynamics*. 2nd ed. Springer.
[4] Gent, P.R. and J.C. McWilliams (1986). "The Instability of Barotropic Circular Vortices". In *Geophysical & Astrophysical Fluid Dynamics* 35.
[5] Storer, B.A., F.J. Poulin, and C. Menesguen (2017). "The Dynamics of Quasigeostrophic Lens-Shaped Vortices". In *Journal of Physical Oceanography* 48.
[6] Ramadhan, A. et al. (2020). "Oceananigans.jl: Fast and friendly geophysical fluid dynamics on GPUs". In *Journal of Open Source Software* 5.

Correspondence: rosalie.cormier@uwaterloo.ca